

Tensile behaviour of unsaturated compacted clay soils — A direct assessment method

Ross A. Stirling^{a,*}, Paul Hughes^b, Colin T. Davie^a, Stephanie Glendinning^a

^a School of Civil Engineering and Geosciences, Drummond Building, Newcastle University, Newcastle upon Tyne, NE1 7RU, UK

^b School of Engineering and Computing Sciences, Durham University, Lower Mountjoy, South Road, Durham, DH1 3LE, UK

*Corresponding author. Tel.: +44(0)1912085268; E-mail: Ross.Stirling@ncl.ac.uk.

Abstract

This paper presents a new method for testing the behaviour of soils placed under tensile load and demonstrates its suitability for testing a number of soil types under various conditions including saturation, compaction and stabilisation. Validation of the results obtained for the soils at relatively low saturation has been conducted using the established Brazilian (indirect) test for measuring the tensile strength of brittle materials. A fair comparison has been found and the results highlight the limited applicability of the Brazilian method to soils at very low water contents at which the tensile failure criterion has been assumed using this methodology. Optical characterisation of the performance of both testing methods has also been conducted using Digital Image Correlation. The consistent, accurate measurement of directly induced tensile strains using the proposed new method has been confirmed, verifying its capability to apply a direct tensile stress in the absence of shearing, a problem commonly associated with other tensile testing methods. The developed technique has then been used to investigate the water content – tensile strength relationship for compacted, unsaturated soils and offers significant advantages in the characterisation of clay soils subjected to variable climatic loading.

Keywords: Compacted clay; Unsaturated clay; Tensile strength; Desiccation cracking; Soil Brazilian testing; Digital Image Correlation

1 Introduction

There is increasing effort being put into the ability to predict the future performance of earthworks and to target resources towards resilient, sustainable maintenance. This is particularly focused in the context of adaptations to our changing climate. The implications of climate on shrink–swelling behaviour are becoming central to the effective management of infrastructure slope assets. It was reported by [Jones and Jefferson \(2012\)](#) that damage due to shrink–swell has cost the UK economy £3 billion in the last 10 years, surpassing that of any geo-hazard. Increased understanding of the changes in performance of engineered fills is vitally important given the wide variety of earthworks assets e.g., embankments, dams, landfill liners and other earth structures. Progressive deterioration of legacy infrastructure leads to serviceability failure and/or serious instability issues. Spatial distribution analysis has indicated that unstable slopes alone with moderate to significant hazard potential constitute up to 10% of the area of Great Britain and that 7% of the transport network is located within this area ([Dijkstra and Dixon, 2010](#)).

Desiccation induces shrinkage that when constrained, due to non-uniform moisture gradients or the presence of any restraining internal soil texture/structure or frictional boundary effect will generate tensile stresses. When these stresses exceed the tensile strength of the material, cracking is initiated ([Corte and Higashi, 1960](#); [Groisman and Kaplan, 1994](#); [Peron et al., 2009](#)). Variability in soil – water content, which governs shrinkage, is primarily the result of seasonal fluctuation in precipitation/evaporation. In addition, soil – water content is affected by the transient demands of vegetation and the infiltration potential of the soil surface. All of these influences are governed by climate. Predicted climate change scenarios are recognised to have

the capacity to more frequently bring about conditions conducive to desiccation cracking because of the tendency towards the increased occurrence of warmer and drier summers (particularly in the South East of the UK) and rainfall events of shorter duration and higher intensity (Hulme et al., 2002; Jenkins et al., 2010). Cracking in geomaterials is a widely researched phenomenon due to its ability to rapidly alter the soil hydraulic properties (Anderson et al., 1982; Albrecht and Benson, 2001; Philip et al., 2002; Romkens and Prasad, 2006; Zhan et al., 2006). The rapid, preferential transmission of water through the full depth of a crack (which can be on the order of metres) is potentially a significant mechanism for strength reduction in earthworks that could lead to earth structure failure. Tensile failure is also reported in clay barriers, where differential settlement of waste material causes cracking and a reduction in liner performance as an effective hydraulic barrier (Jessberger and Stone, 1991). Chemically modified/cement stabilised materials in road and rail line sub bases can also undergo tensile cracking induced by traffic generated cyclic stresses.

Tensile strength plays a vital role in the understanding of soil cracking as it becomes increasingly unsaturated. Tensile strength is the product of real cohesion (natural or artificial cementation between particles) and apparent cohesion due to suction (Lakshmikantha et al., 2012).

Tensile strength is often over looked and is difficult to determine using the traditional suite of standard laboratory tests. Therefore, the ability to characterise the tensile strength/stiffness behaviour of geomaterials is of great importance to engineering geologists and geotechnical engineers.

There exist a number of methodologies available for the characterisation of the tensile strength of geomaterials. These can be separated broadly into two categories; direct and indirect tests. Direct tests are classified as using an applied axial tensile load and indirect tests as exploiting the application of non-tensile loading (e.g. compression) such that the specimen fails in tension. Direct tests include modification of triaxial testing apparatus (Tang and Graham, 2000; Heibrock et al., 2005; Zeh and Witt, 2007) and modification of direct shear testing apparatus (Nahlawi et al., 2004; Tamrakar et al., 2005; Trabelsi et al., 2012). Indirect tests include the Brazilian tensile test (Frydman, 1964; Krishnayya and Einsenstein, 1974), Hollow Cylinder Triaxial test (Alsayed, 2002) and beam bending (Thusyanthan et al., 2007). Each of these approaches has advantages and limitations. The Brazilian tensile test is only suitable for relatively stiff material and therefore cannot be reliably used to test saturated clay soils that exhibit plastic behaviour. Hollow Cylinder tests require complex specimen preparation due to their hollow geometry. The preparation of beam bending specimens is relatively simple; however, results are sensitive to specimen and loading geometry in addition to strain rate. Modification of a standard triaxial testing system, such as that by Zeh and Witt (2007), requires complex specimen preparation in which a textile fabric drain is placed down the centre of the specimen, risking damage in the process. Direct testing of rectangular, bow tie or dog bone shaped prisms involves less complex specimen preparation but there is the potential for squeezing of low stiffness material by shear keys and loading jaws leading to uneven stress distributions and inaccurate measurement.

The research presented in this paper describes the development of the Newcastle Direct Tensile Test (NDTT) methodology that is based on a simple reversible modification of existing standard geotechnical laboratory equipment. The results have been validated against those obtained using classical tests for (brittle) geomaterials. The Brazilian test was developed for the assessment of brittle materials and has been shown to be applicable for soils in limited, low saturation conditions (Frydman, 1964; Krishnayya and Einsenstein, 1974). Furthermore, full-field strain distribution across specimens has been monitored using Digital Image Correlation (DIC) during testing to investigate the generation of inferred tensile stresses. The application of this technique to assess tensile strain development has been established in direct (Divya et al., 2014) and indirect (Stirling et al., 2013) tensile testing.

2 Method

2.1 Materials

Three soils at a range of moisture contents were selected for testing in order to assess the direct and indirect tests across a range of applications. These consisted of commercially available kaolin–bentonite–sand (KBS) mixture, remoulded glacial till and cemented silty sand. Table 1 shows the classification properties of these materials; liquid limit, L_i , plastic limit, P_i , plasticity index, PI, optimum moisture content (at which maximum dry density is achieved) and the Particle Size Distribution (PSD) coefficients of uniformity (C_u) and curvature (C_z).

Table 1 Material classification parameters (conducted in accordance with BS 1377 Parts 2 and 4).

	L_i (%)	P_i (%)	Plasticity Index (%)	*Optimum Moisture Content (%)	*Maximum Dry Density (Mg/m^3)	PSD	
						C_u	C_z
KBS	34	16	18	16	1.76	17.3	6.1
Glacial till	45	24	21	15	1.82	9.6	1.2
Cemented silty sand	23	11	12	11	2.00	18.7	5.8

*Conducted using the 2.5 kg rammer method (British Standard Institute, 1990b).

The KBS soil was used in evaluation of the NDTT loading jaw design and the applicability of indirect testing on specimens at relatively high water content through the use of Digital Image Correlation. The composition by dry weight was kaolin 47.5%, sodium carbonate activated bentonite (mainly sodium and calcium montmorillonite) 2.5% and sharp sand 50%. The kaolin mineralogy is described as kaolinite with minor amounts of mica, quartz and feldspar or illmenite, chemical analysis by X-ray fluorescence showed SiO_2 50% and Al_2O_3 35% by dry mass (IMERYYS, 2008). An artificial, cemented soil comprising silica sand 67.5%, kaolin 27.5% and CEM-1 5%, was used to demonstrate the range of applications for which the direct test may be used and to aid in the comparison of test methods. The remoulded glacial till represented a common engineering fill material used in the construction of, among other applications, infrastructure slopes. As this material originates from a natural deposit, XRD analysis was conducted. The following composition was established: quartz 63.5%, feldspar 7%, phyllosilicates/clay minerals including undifferentiated mica species 18.2%, kaolinite 7.1% and chlorite/smectite 0.7%.

2.2 Direct tensile testing

The fundamental principle behind the apparatus is that direct tensile stresses are measured via a simple, easily reversible modification to the standard direct shear strength test, BS1377-7 (British Standard Institute, 1990c). In this way, the means of both generating and measuring load are already established. The rig chosen for modification was a conventional Wykham Farrance 60 mm square direct shear testing rig.

Several designs of jaws/platens have been proposed by previous authors including internally or externally glued fixings (Heibroock et al., 2005) and friction based designs such as truncated cylinders (Tamrakar et al., 2005) and truncated triangular prisms (Rodriguez, 2002; Kim and Hwang 2003; Trabelsi et al., 2012). In order to induce tension, a pair of loading jaws was designed between which the soil specimen is mounted. No adhesive was used in an effort to avoid the introduction of any additional media as it is thought that this may influence the measurement of tensile stress and complicate the quick and easy production of test specimens. A friction based system was selected and is shown in Fig. 1. Specially designed rigid PVC jaws that grip the specimen (Fig. 1a) were constructed and mounted together into the standard direct shear carriage (Fig. 1b). An interior jaw angle of $\sim 20^\circ$ was used in accordance with Arslan et al. (2008) and Kim and Sture (2008), as reported by Divya et al. (2014). This angle is recognised to be greater than the potential dilatancy of any material tested in this work and is thought to prevent the relative displacement of soil particles with respect to the confining jaw surface resulting in a uniform distribution of compressive stress.

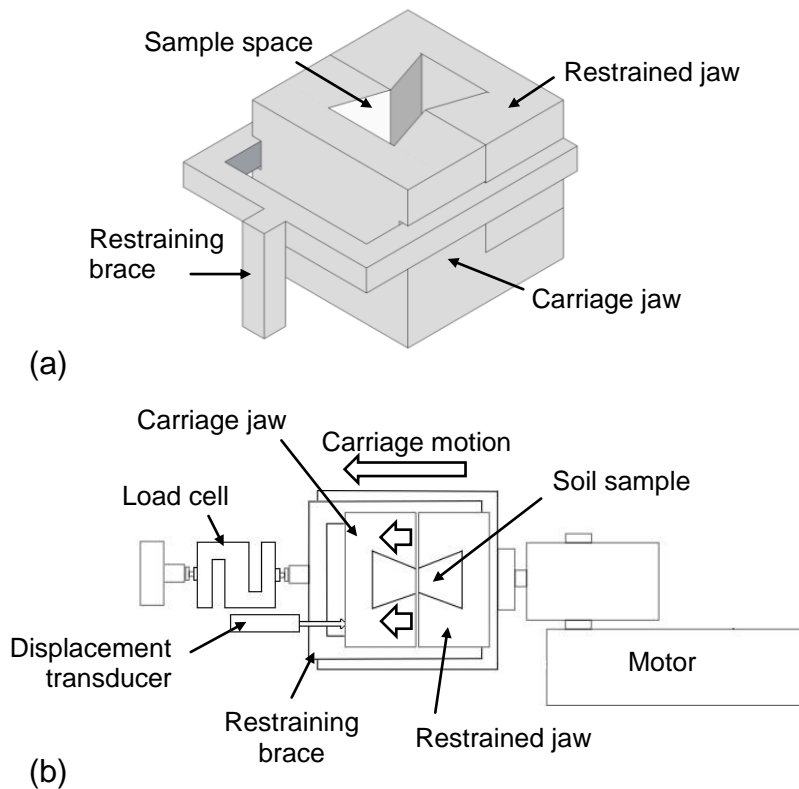


Fig. 1 Tensile test equipment (a) loading jaws and (b) schematic of testing rig (Stirling et al., 2014).

Crucially, the jaws are made to separate in a uniaxial manner at an adjustable, constant rate. To achieve this, the jaws are placed within the carriage that is propelled by the motor; however one jaw is restrained by a brace (restrained jaw, Fig. 1 a). Hence, the carriage jaw is made to move along greased bearings relative to the restrained jaw. As the carriage jaw is propelled, load is transferred evenly through the cross-section of the specimen to the restrained jaw. A brace element allows the load to be transmitted to the load gauge positioned at the opposite end of the rig. The specimen possesses a mirrored isosceles trapezium plan cross-section ($38 \times 54 \times 50$ mm (78.3 ml volume)) that aids the constraint of the specimen and induces failure at the centre due to the reduced cross-sectional area.

The natural soil was prepared by air drying to residual moisture content before being passed through a 5 mm sieve. This process is known to alter the natural PSD of the natural glacial till material; however, it was deemed impractical to test soils whereby individual grains constituted greater than 2% of the total volume of the specimen. This procedure is in accordance with the preparation of direct shear (shearbox) specimens (BS1377-7:1990) sub-section 7.7.2 where the maximum particle size is given by $H / 10$ where H is the specimen height taken as perpendicular to the shear plane (British Standard Institute, (1990c)). Following drying, de-ionised water was then added to bring the soil to predetermined water content and the bulk specimen was then wrapped in uPVC film and left to equilibrate for at least 24 h. After this period, a sub-specimen of soil was weighed so that when using the purpose built steel press, a specimen of the desired density was produced. This process allowed the rapid production of specimens with consistent water contents, densities and dimensions.

Where required, subsequent drying of specimens was achieved through air drying until the desired water content was reached as determined by gravimetric means. Some volume change resulted from this process, although it was considered negligible. Specimens were then re-sealed for 24 h to allow an even re-distribution of water within the specimen prior to testing. Cemented soil specimens were sealed and allowed to cure in a temperature controlled room (at 22 °C, 55% humidity) for 7 and 21 days before being air dried in the same way.

Direct tensile testing was conducted on all the soil types listed in Table 1. Specimens were placed in the loading jaws and a constant strain rate applied. Load transmitted through the specimen was recorded continually until the two halves of the specimen were completely separated and the load

reading returned to residual values. It must be noted that non-zero stress values are recorded post specimen failure indicating, as in any mechanical system, a level of internal system friction/inefficiency.

A range of displacement rates are available by using an existing direct shear rig. A series of constant applied rates were used in production of the presented results and are expressly stated in the results section as these are specific to each study undertaken. The effect of strain rate on measured tensile stresses using the direct apparatus was investigated and it was found that lower rates (e.g., 0.24 mm/min) produced a higher repeatability than higher rates (e.g. 1.22 mm/min) in addition to a lower degree of data scatter in drier specimens (Davies, 2012). However, little difference was seen with respect to the overall tensile strengths recorded. The testing conditions are provided in Table 2.

Table 2 Specimen conditions used during direct tensile testing.

Soil type	Water Content at compaction (%)	Water Content tested (%)	Number of specimens	Mean Dry Density (Mg/m ³)
KBS	23	23-5	53	1.65
Glacial Till	23	23-2	35	1.56
Cemented Silty Sand	15	13-1	8	1.87

Specimen preparation required approximately 20 min of operator time per specimen, although when created in large batches this substantially reduces. The tensile test itself took approximately 25 min per specimen from mounting to recovery for post-testing moisture content checks. Initial fitting of the tensile test adaption to the shear box equipment takes approximately 5 min and a similar length of time was required to remove the apparatus and return the shear box to its original use once testing was concluded.

2.3 Indirect tensile testing

In the absence of a standardised tensile strength test for soils, the Brazilian test was used as a means of comparing results obtained from the developed NDTT. The application of the Brazilian test to determine the tensile strength of any material requires a number of assumptions: that the material behaves with biaxial linear elasticity in two-dimensions and is homogeneous and isotropic in terms of its strength and elastic properties. It is these assumptions that rule this method inappropriate for use on saturated soils. However, as discussed by Frydman (1964), when soils are in an appropriately brittle condition, the method may be justified. The aforementioned three soil types were used for the purposes of Brazilian testing. In order to best meet the assumptions of the Brazilian test, the soils were tested at low water contents where elastic behaviour is most pronounced.

Brazilian test specimens were formed from soils manually compacted into 100 mm diameter cylinders. The same dry densities as specimens tested in parallel using the direct method were chosen to allow for a fair comparison. Likewise, the same water content at compaction was used for each specimen type i.e., specimens tested indirectly and directly possessed the same dry density. The compacted soil was allowed to air dry until considered suitable for dry cutting. Disc specimens were cut to a thickness-to-diameter ratio of 0.5 (within the ASTM recommended 0.2–0.75 range). At this point, half of the discs were then wrapped in plastic film and left to equilibrate for 24 h. The remaining discs of each soil type were allowed to continue drying for a further 7 days until residual water content was reached before being wrapped and allowed to equilibrate. Cemented soil cylinders were wrapped immediately after compaction and left to cure for 7 and 21 days prior to air drying, in the same manner as specimens produced for direct testing. As in production of direct testing specimens, two curing times were chosen to provide two specimen sets of differing tensile properties due to cementitious bonding. Cemented soil discs were cut and tested within a 4 h interval.

The Brazilian test method adopted herein is that of the ASTM D3967 -08 (ASTM, 1984) whereby the disc shaped specimen is diametrically loaded upon its circumference via the use of flat platens. As recommended by the ASTM (1984), a constant rate of loading such that the specimen fails between 1–10 min was employed. This was back-calculated from tensile strengths obtained during preliminary testing. On average, all tests took 7–8 min from initial loading to failure. Compression loading was

provided using an Instron 5585H universal testing machine fitted with platens conforming to section 5.2.1 of ASTM D3967-08. The specimen specific loading rates are provided alongside the general test conditions in Table 3. Mean water contents stated represent those established immediately following the completion of each test.

Table 3 Brazilian test conditions.

Test #	Material	Mean water content (%)	Mean dry density (Mg/m ³)	Curing time (days)	Loading rate (kN/min)	# Tests conducted
1	KBS	7.4	1.65	-	0.12	3
2	KBS	15.2	1.65	-	0.06	4
3	Glacial till	5.7	1.56	-	0.20	3
4	Glacial till	17.9	1.56	-	0.12	4
5	Cemented soil	1.0	1.87	21	0.10	3
6	Cemented soil	13.1	1.87	7	0.06	4

Specimens were loaded until brittle failure was observed by way of vertical fracture across their diameter. Following ASTM guidance, tensile strength was calculated from P, the load corresponding to failure and the thickness, t and diameter, D, of the specimen according to $\sigma_t = 2P/\pi Dt$.

The failure load is defined as the maximum applied load measured and was recorded immediately prior to the abrupt loss of stiffness where it is no longer possible to maintain a constant loading rate. It is important to note that up until this failure load, the specimen is believed to be fully intact and may therefore be assumed to behave linear elastically.

2.4 Digital Image Correlation

Digital Image Correlation (DIC) is an optical method that uses surface deformation tracing and registration to distinguish changes in an applied speckle pattern and correlate them to measurements of strain in 2D. The theory behind DIC was first suggested by [Chu et al. \(1985\)](#) and has subsequently been applied to many areas of material testing. The non-invasive technique was employed to measure the full strain field across the surface of KBS specimens during direct tensile testing due to the pale kaolin-based soil providing the perfect contrasting colour on which to apply the necessary speckle pattern required ([Fig. 2](#)). This was carried out to investigate the development and distribution of strains during loading. However, it is necessary to assume specimens to be homogenous when considering the extrapolation of surface strain to any depth internally.

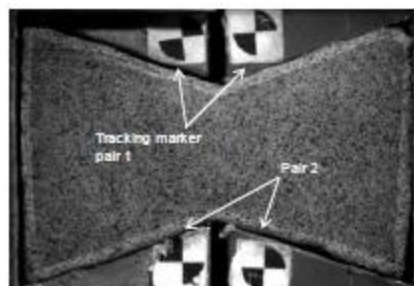


Fig. 2 Specimen showing speckle pattern and tracking markers.

The DIC hardware setup and specimen preparation is crucial in the recovery of useful and accurate strain data. In direct tensile testing, two high resolution cameras were positioned symmetrically 300 mm above the specimens on a tripod and profile bar approximately 150 mm apart. Telephoto lenses of 28 mm focal length and a 2 mm relative aperture were fitted to the cameras. To prepare specimens for monitoring, a black-on-white speckle pattern was applied to the upper surface of the specimens using fine aerosol paint. This pattern was both non-repetitive and isotropic ([Correlated Solutions, 2010](#)). Additional LED (cold source) lighting was set up to ensure sufficient contrast of the speckle pattern was maintained. To minimise the effects of motion blur, exposure was set to a minimum (26 ms) with the aperture increased to compensate for the reduced light input. Following full calibration,

the images were captured automatically at a frame rate of 5 frames per second (200 ms intervals) during testing.

After testing images were captured they were then analysed using VIC-3D software to generate contour plots of the 2D strain field (Correlated Solutions, 2010). An area of interest was then defined on the pre-deformation, reference image consisting of a subset of 45 × 45 pixels and used for all analyses due to the consistent speckle pattern. Since fracture is expected to occur across the centre of the specimen, two analysis 'seed points' were used to ensure a continuous analysis across as much of the specimen surface as possible including post-fracture.

In addition to using the DIC system to map the full-field strain development on the 'bowtie' specimen surface during testing, the mechanical behaviour of the loading jaws was recorded. Displacement of the jaws themselves was tracked relative to markers placed in strategic locations (across jaws and within the captured field of view) shown in Fig. 2. These markers have been tracked in post-processing giving an indication of jaw separation behaviour.

The DIC technique was also used to evaluate the validity of the indirect tests conducted on KBS disc specimens. A configuration similar to that adopted to monitor direct testing was setup comprising a camera separation of 249.0 mm with a distance of 276 mm from the specimen position and with an exposure of 42.5 ms; image capture was conducted at an interval of 500 ms.

3 Results

3.1 Direct testing

The stress–strain results for tests conducted on the KBS material at 1.22 mm/min are presented in Fig. 3. It can be seen that stress increases somewhat linearly with evidence of softening immediately prior to reaching peak stress. Beyond the ultimate strength, the specimens are found to fail in the form of a tear across the neck of the specimen. In dryer specimens (below plastic limit), the stress is shown to drop more sharply. However, in wetter specimens (above plastic limit) a strain softening behaviour is apparent post-failure. This is shown by the gradual decrease in stress with continued strain until returning to the residual system value. These specimens exhibit a less well defined brittle fracture and eventually divide following a period of minor neck thinning.

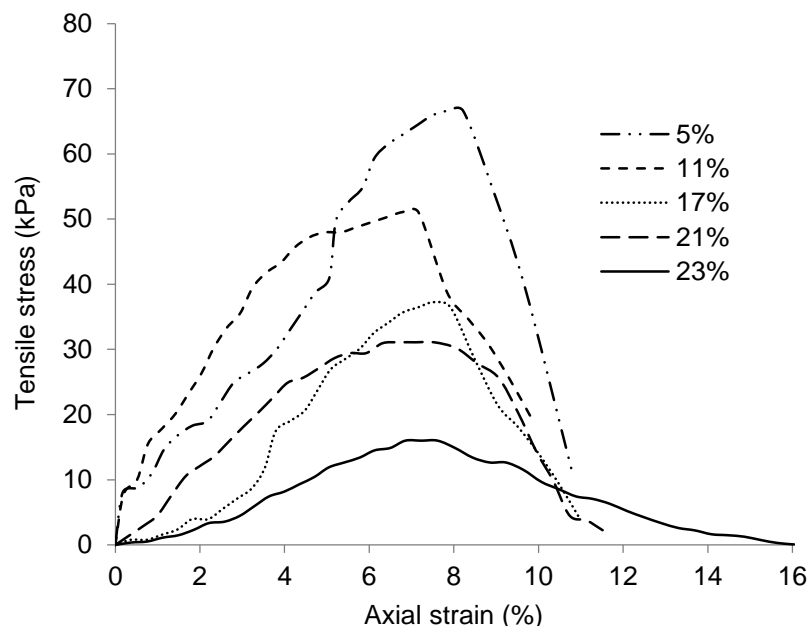


Fig. 3 Tensile stress–strain results for KBS soil at varying moisture contents.

The results for tests conducted on the glacial till, also at a strain rate of 1.22 mm/min are shown in Fig. 4. This material exhibits greater tensile strengths than the KBS mix. Although similarly, the tensile stress–strain relationship can be seen to be approximately linear with specimens at the drier end of the moisture content range failing in a very well defined brittle manner. Hardening behaviour is observed immediately prior to peak stress in specimens at lower water content. However, a more

pronounced difference in tensile behaviour due to the influence of water content is captured than in the homogeneous KBS material.

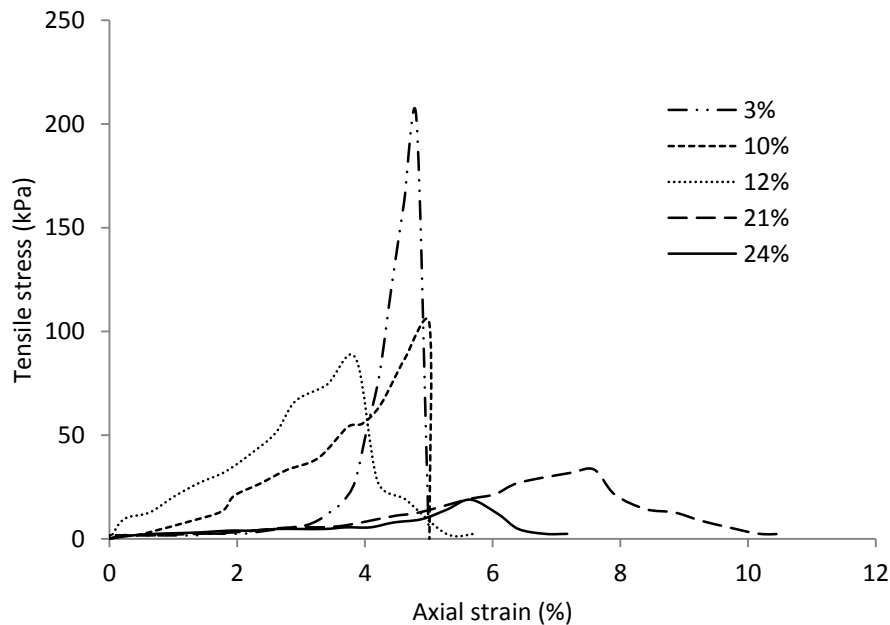


Fig. 4 Tensile stress–strain results for glacial till at varying moisture contents.

In addition, specimens of glacial till were tested in order to establish the relationship between soil–water content and tensile strength as the soil dries (shown in Fig. 5). These tests were conducted at a displacement rate of 0.24 mm/min. The plot shows an exponential increase in tensile strength with reduction in water content and progressively larger variation in tensile strength measurements at lower water contents. However, a fairly clear relationship can be seen despite these variations.

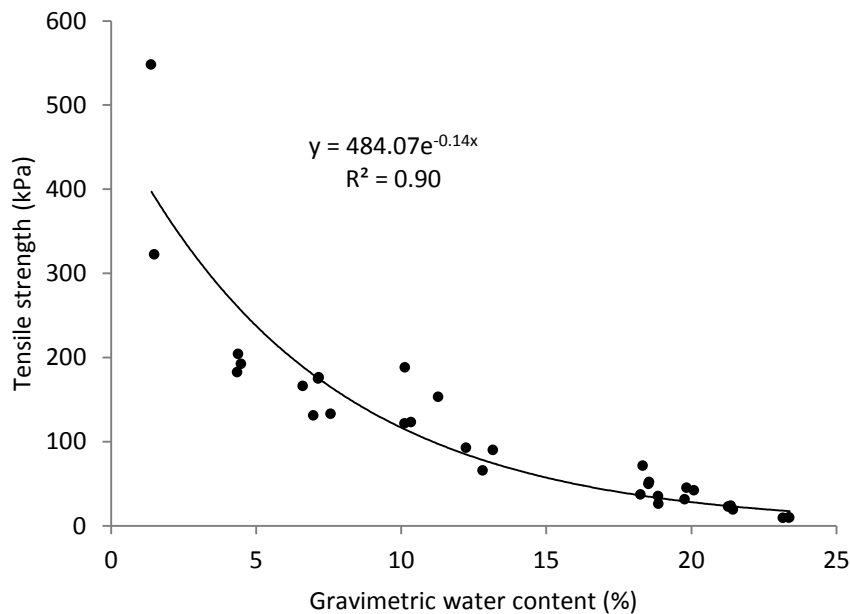


Fig. 5 Tensile strength as a function of water content for the glacial till.

This is consistent with the work by many researchers (e.g., Nahlawi et al., 2004; Zeh and Witt, 2007). According to the two-part classification of tensile strength by Lakshmikantha et al. (2012), strength experienced at relatively high water content is likely attributable to real cohesion with an increased influence of suction with progressive de-saturation. The change in water content over the experimental range is unlikely to be influential in the real cohesion component of tensile strength but

instead be subject to the generation of suctions up to the order of 10 MPa. At the bounding moisture contents of cemented soil testing, higher tensile strengths were measured than at low contents though the mechanisms through which these strengths are generated also relate to the formation of hydrated cement minerals such as calcium silicate hydrates and calcium aluminate hydrates. Therefore, if the specimens were re-wetted, one would not expect the same reductions in strength as in the untreated clay soils.

A total of 50 tests conducted on the KBS material were monitored with DIC and the images analysed using VIC 3D software. A specimen analysed at 20% water content with a displacement rate of 1.22 mm/min is presented in Fig. 6. It may be seen that tensile strain is initiated at approximately 120 s into the test and originates at the lower vertex. After 180 s a band of tensile strain is seen to have developed across the central portion of the specimen between the vertices of the carriage jaw. However, at 228 s a secondary tensile strain localisation is seen to have formed at the lower vertex of the restrained jaw. It is this concentration that is seen to develop into the site of eventual fracture after 240 s. Fracturing manifests itself as gaps in the contoured data where correlation is not possible due to disintegration of the speckle pattern. The final fracture formation is shown in the photograph at 258 s (Fig. 6h). This series illustrates the localisation of tensile strain across the centre of the specimen though the influence of jaw vertices on the initiation of fracture in a wet of optimum specimen is highlighted. Little compressive strain is seen to have developed adjacent to the jaw interior suggesting that the clamping effect is well distributed outside the central specimen area.

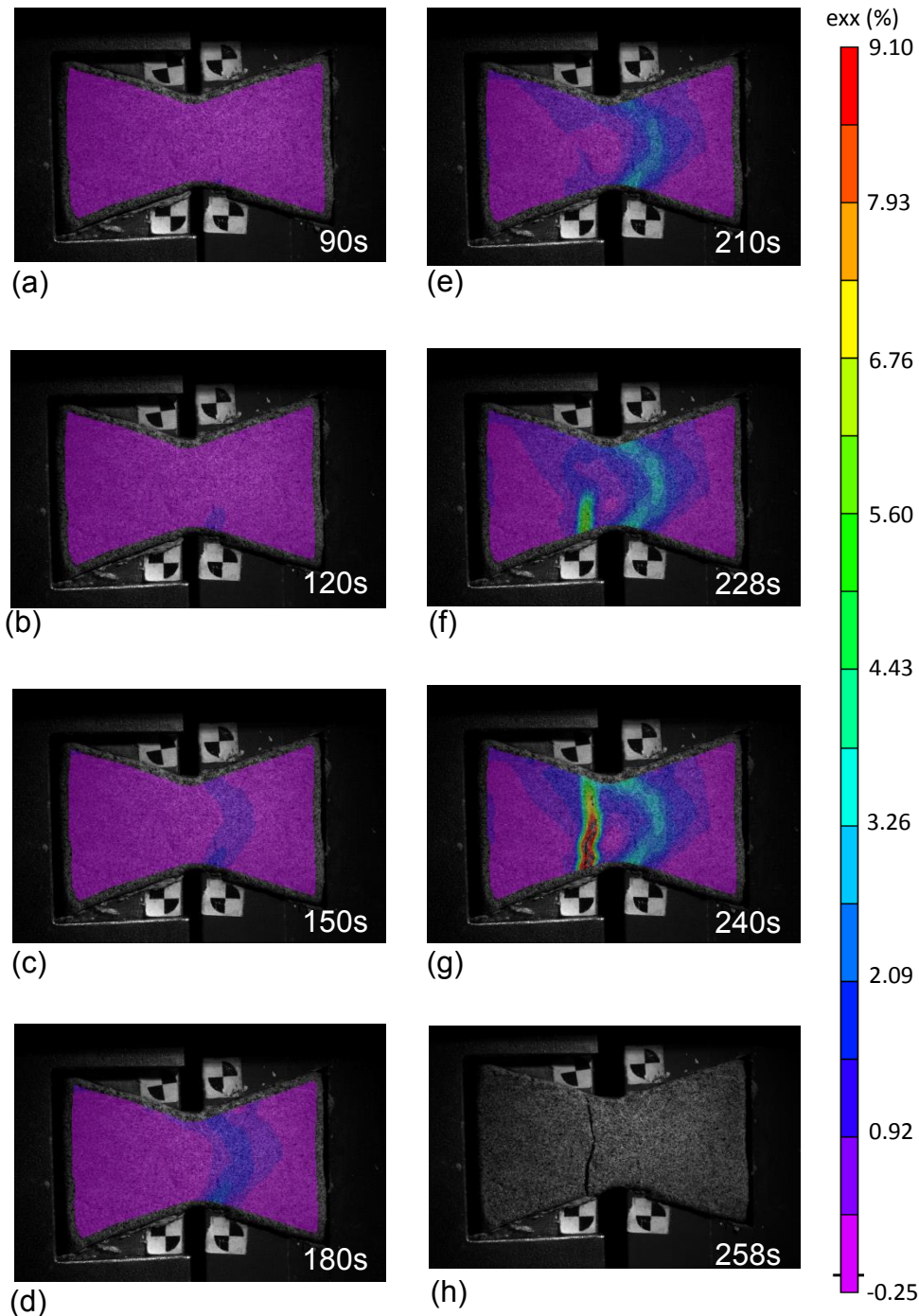


Fig. 6 xx strain distribution in a specimen tested at 20% water content.

The same displacement rate was applied to a specimen at 10% water content and is presented in Fig. 7. Beginning at 300 s into the test, strain is observed to develop across the specimen in a similar manner to Fig. 6. However, additional strains are seen adjacent to the restrained jaw interior. This is thought to be associated with the alignment of the specimen within the jaw space and is discussed later with the aid of data obtained using tracking markers. At 336 s, tensile strain is found to have localised about the narrow section of the 'bowtie'. Importantly, this behaviour is shown to develop symmetrically about the axis of loading. From 342 s fracture is observed to propagate towards the centre of the specimen until full separation is achieved at 360 s.

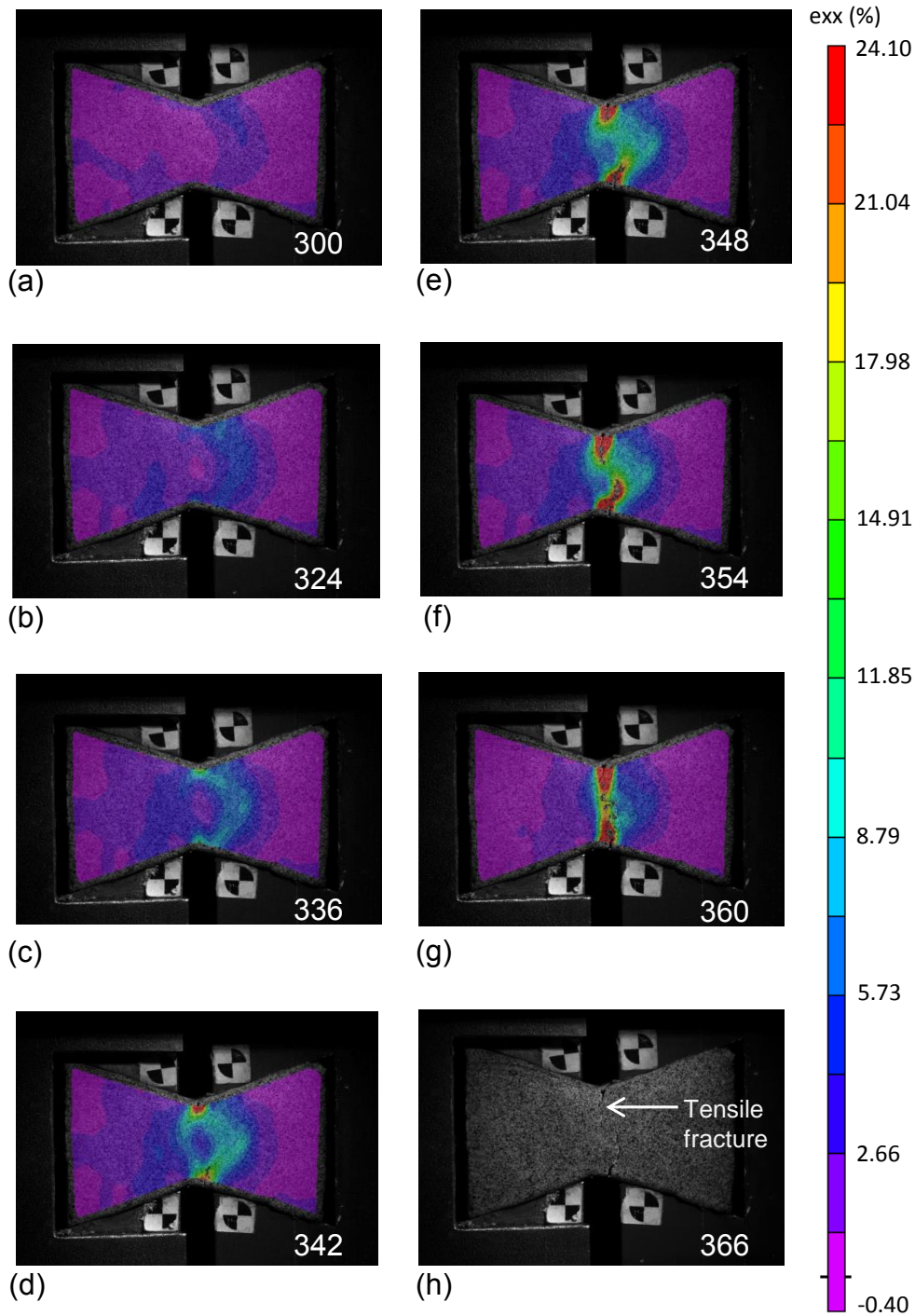


Fig. 7 xx strain distribution in a specimen tested at 10% water content.

The difference in x-displacement between the two jaws for a series of tests on the KBS soil was calculated using tracking data taken at the top (1) and bottom (2) marker pairs shown in Fig. 2. Tracking at the top and bottom was undertaken to investigate the parallelism of the motion of the carriage jaws and the true rate of applied strain. Direct tension was induced in specimens compacted at 22% water content using a motor rate of 1.22 mm/min. Representative tracking results are presented in Fig. 8 alongside the constant, idealised motor displacement.

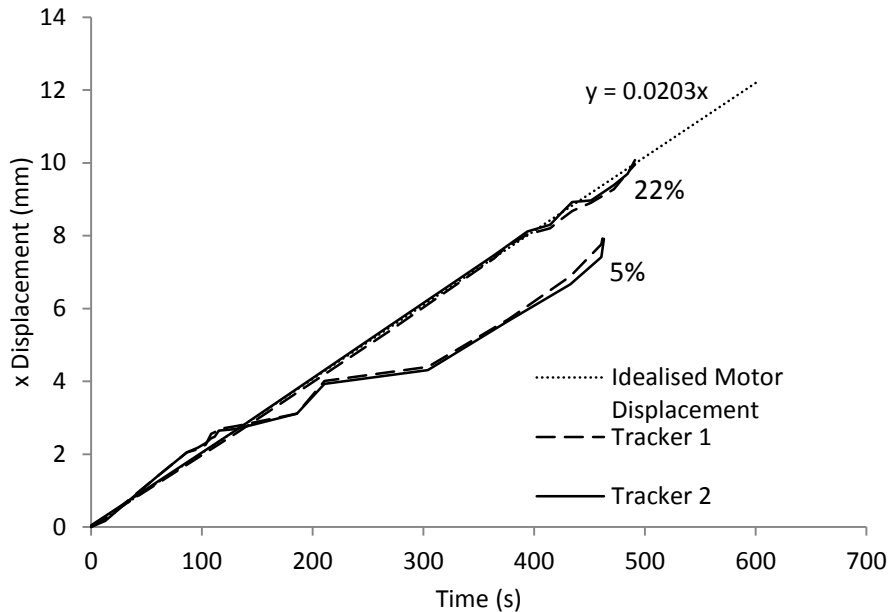


Fig. 8 Jaw marker displacement.

From the tracking data recorded during the testing of a specimen at the as-compacted water content, it can be seen that the displacement of both sides of the carriage jaw is identical to the input motor speed for the majority of the test. This confirms that the applied motor rate is being translated into specimen strain and that the jaws are parting in a perfectly uniaxial manner. The relatively weak, saturated material showed little resistance to the separation of the loading jaws and is noted to fit within the jaws with very little spare space i.e., full soil-jaw contact from the start of jaw motion. Specimen failure correlates to approximately 400 s where the tracked displacement is seen to deviate from that of the motor speed. The final portion of the tracking data shows an increased displacement rate. This is brought about by the softening of the soil linkage between the two jaws after failure and displacement recovery. The plot shows that the jaws are behaving correctly throughout the test up to the point of failure. There is very little misalignment in the path of the jaws and the specimen is undergoing the desired strain rate.

In contrast, tracking data for a specimen dried to 5% water content is seen to deviate from the intended motor speed after approximately 60–120 s. At 120 s the two sides of the carriage jaw show a brief difference in displacement. This is considered to be the product of specimen re-alignment occurring when the specimen comes into contact with the interior of either jaw having previously been free. The freedom of the specimen during the initial portion of the test is a trait of specimens tested in the drier condition. As part of the drying process, the clay specimens underwent some free, isotropic shrinkage leading to space between the untested specimen and the loading jaws. The reduced displacement rate evident at 115–185 s indicates a resistance to jaw separation due to the higher stiffness of the drier soil state. At 185 s the rapidly increased displacement is the result of slippage between the specimen and the interior of the jaw. Another alignment event at approximately 210 s sees the stiffness of the specimen again reduce the rate of jaw separation. Full specimen-loading jaw contact is observed for the remaining time of the test. However, the even displacement of the jaws diverges slowly at 305 s. Divergence is indicative of non-uniform jaw separation where one side of the specimen is either able to slide against the interior jaw wall or fracturing of the specimen has initiated at one side of the centre section. In the case presented in Fig. 8, fracture has initiated at the top edge seen as a rate increase at tracker pair 1. The fracture continues to propagate until full separation is achieved at approximately 460 s when both sides of the jaw rapidly and simultaneously increase in displacement rate. The period of full specimen contact and therefore loading is found to be relatively short in comparison to the testing at 22% water content, as would be expected for a more brittle material. The ability to assess jaw alignment during testing is restricted to the use of tracking technology, an otherwise complicating procedure in the pursuit of a quick and simple tensile testing method. However, the facility to directly measure true carriage jaw displacement constituted an advance in confidence when applying the NDTT method.

3.2 Indirect testing

The average tensile strengths of each soil type under the six saturation conditions are provided in [Table 4](#). Load and vertical strain data recorded externally using the testing rig load cell and displacement transducer for representative tests of each specimen condition are presented in [Fig. 9](#). Load take-up and post-failure data have been removed for clarity.

Table 4 Results of Brazilian tests.

Test #	Material	Mean water content (%)	Mean failure load (kN)	Mean tensile strength (kPa)	Standard deviation (%)
1	KBS	7.4	0.91	116.00	5.74
2	KBS	15.2	0.62	79.20	14.51
3	Glacial till	5.7	1.62	206.77	20.26
4	Glacial till	17.9	0.52	66.24	11.87
5	Cemented soil	1.0	0.71	90.74	3.52
6	Cemented soil	13.1	0.40	50.81	8.84

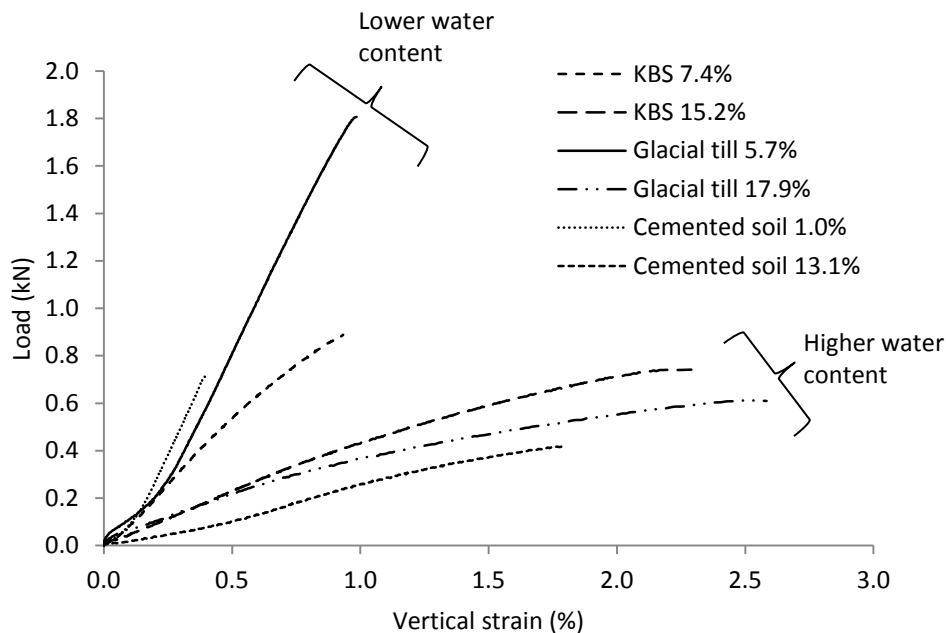


Fig. 9 Representative load – vertical strain relationships for all test conditions.

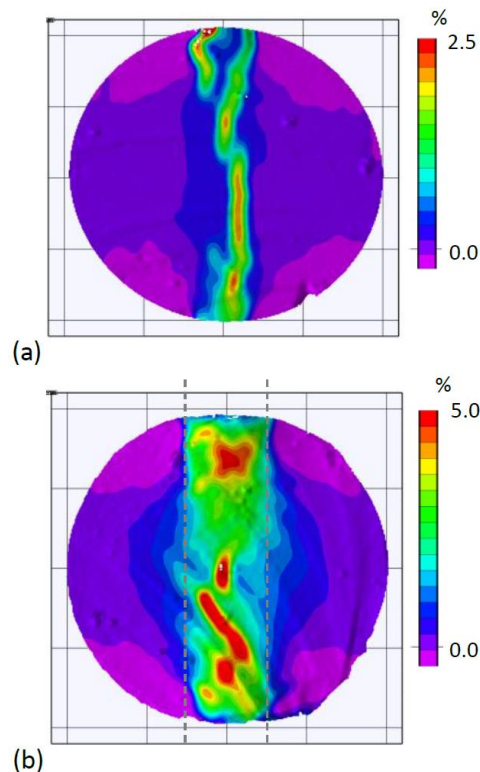
It may be seen that there are two dominant trends in the load–strain behaviour, as indicated in [Fig. 9](#). Specimens tested at the lower water contents exhibit a relatively stiff response to loading and show a broadly linear trend. This is with the exception of ‘KBS 7.4%’, the wettest of the low water content specimens which is seen to deviate from a linear elastic trend beyond 0.6% strain. These drier specimens were found to fail at higher compressive loads than those specimens at higher water contents. However, wetter tests show an increasingly softer, plastic response with increased loading.

For the purposes of DIC, high-resolution images were captured of specimens under test condition 1 ([Table 4](#)), denoted ‘D’ and test condition 2, denoted ‘W’. The results of individual tests are presented in [Table 5](#). A clear difference is shown between the average tensile strength magnitudes of the respective states.

Table 5 DIC test IDs and results.

Test ID	Water content (%)	Tensile strength (kPa)
D1	8	112.26
D2	6	113.14
D3	9	122.62
W1	16	60.83
W2	14	94.44
W3	15	86.10
W4	16	75.40

Beyond the clear difference in strength, DIC has provided evidence for the contrasting manner in which tensile strains are developed during application of vertically compressive load. Representative contour plots showing full-field strains immediately prior to failure (< 500 ms) are provided in Fig. 10. The apparent near-perfectly circular geometry of test D2 (Fig. 10a) indicates little to no platen-disc contact deformation and the generation of a narrow, constrained region of tensile straining. Although approximately four regions of elevated xx strain may be discerned, it is not possible to definitively determine the location of failure initiation. However, the alignment of these regions suggests at least a horizontally centralised failure initiation. In contrast, the plot showing test W2 (Fig. 10b) displays a high level of disc distortion in the lead up to failure. This is manifested as apparent flattening of the disc at platen contacts. The broadening of this contact area results in similar broadening of the diametric tensile region. This acts to relieve the focused stress associated with the platen-disc point of contact and so the position of elevated tensile strains in this case is away from the loaded circumference. A similar behaviour was observed by Stirling et al. (2013) in the comparison of strain generation between the use of circular (ASTM, 1984) and flattened rock disc geometry testing (Wang and Xing, 1999). Strain magnitudes of approximately double that seen in D2 were generated before failure, although as was presented in Table 5, ultimate tensile stress was observed to be consistently lower in the tests nearer to saturation.

**Fig. 10** xx strain distribution immediately prior to failure in Brazilian specimens tested at (a) 6% and (b) 14% water contents.

As described by Frydman (1964), when performing Brazilian tests on soil discs, appreciable deformation occurs at the point of loading in the form of flattening; a plastic behaviour. It was proposed that elasticity still be assumed throughout due to plastic deformation being confined to the loaded circumference and not dominating the centre of the disc where the critical tensile stress is generated and indirectly calculated.

Acknowledgement of expected disc deformation is required to assess the validity of the classic relationship. Frydman (1964) concluded that the tensile stress generated in the centre of the deformed disc is given by Eq. (1). The term $g(\sigma_x)$ acts to factor the standard expression for tensile stress by relation to the half width of the flattened, loaded area of the disc, a , and the half distance between these flattened areas, y_1 .

$$\sigma_x = g(\sigma_x) \frac{2P}{\pi Dt} \quad 1$$

where,

$$g(\sigma_x) = -\frac{D}{2a} \left\{ 2f - \sin 2f - \frac{2y_1}{D} \log \tan \left(\frac{\pi}{4} + \frac{f}{2} \right) \right\} \quad 2$$

where,

$$f = \tan^{-1} \frac{a}{y_1} \quad 3$$

It follows that as the ratio between the width of the flattened area and the distance between them increases, the non-factored condition is approached. Frydman (1964) asserts that should this ratio be ≤ 0.27 then it is appropriate to assume $g(\sigma_x) = 1$ within the accepted accuracy of the test. The high rate photography used in the DIC process enabled dimensions of the discs immediately prior to failure (< 500 ms) to be recorded. Widths were measured at the upper and lower loading points and averaged while the distance between the flattened ends of the discs was extracted from platen displacement data. The geometric data relating to the Frydman criterion is presented in Table 6.

Table 6 Frydman Brazilian test validity data.

Test ID	Water content (%)	Flattened area width (mm)			Distance between flattened areas, $2y_1$ (mm)	y_1/a
		Upper	Lower	Mean, $2a$		
D1	8	7.68	12.45	10.07	1.24	0.12
D2	6	11.88	12.32	12.10	0.93	0.08
D3	9	13.39	12.76	13.07	1.68	0.13
W1	16	29.01	28.98	29.00	6.02	0.21
W2	14	16.99	15.69	16.34	2.44	0.15
W3	15	22.53	19.45	20.99	3.39	0.16
W4	16	25.19	23.02	24.10	4.78	0.20

The ratio y_1/a used to describe the degree of soil disc deformation can be seen to correlate well with the water content of each specimen, where lower ratios are found for drier specimens showing more brittle behaviour. It is noted that all test ratios remain below the 0.27 value and therefore the classic tensile strength expression stated in the ASTM and ISRM standards has been used. However, the full-field strain data has demonstrated the great influence water content has on the plastic deformation of the disc and the validity of calculated tensile strength values is considered questionable.

4 Comparison

In order to evaluate the consistency of directly measured data with other, recognised methods of geomaterial tensile strength testing, comparable specimen states were subjected to Brazilian (indirect) testing. All three soil types, KBS mix, glacial till and cemented silty sand were tested

according to the indirect method ASTM D3967-08. Additional specimens were formed for direct tensile testing from the same mix to guarantee consistency between the different specimen types. A comparison of the results obtained from the Brazilian tests and the direct tensile tests is presented in Fig. 11. The figure shows that the results compare well between the two types of test. Generally, the direct tensile test does not consistently over or under-estimate the tensile strength when compared to the Brazilian test across the range of soil and water contents. The maximum difference in measured strength is 26.6 kPa shown by glacial till at 18% followed by 10.6 kPa for the KBS mix at 15% water content. Cemented soil displays very little difference between test methods at the high water content. Hence, results exhibit the most uncertainty at higher water contents and this potential overestimation increases according to an increase in plasticity index.

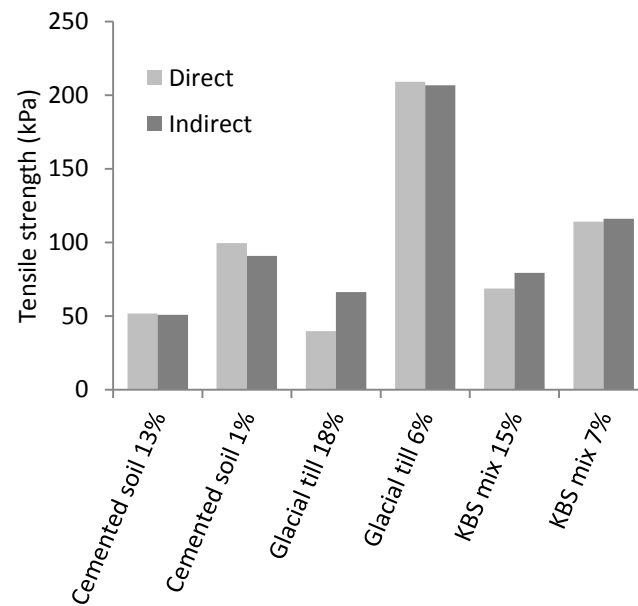


Fig. 11 Comparison of results from Brazilian test and NDTT for a selection of soil types at common percentage water contents.

In addition to comparing the ultimate tensile strengths between the two tests, by establishing the unconfined compressive strength (UCS) – water content relationship for the glacial till, it has been possible to evaluate behaviour of direct and indirect tests conducted at ‘high’ and ‘low’ water contents in Mohr space. The UCS – water content relationship was defined by a linear expression from the data presented in Fig. 12.

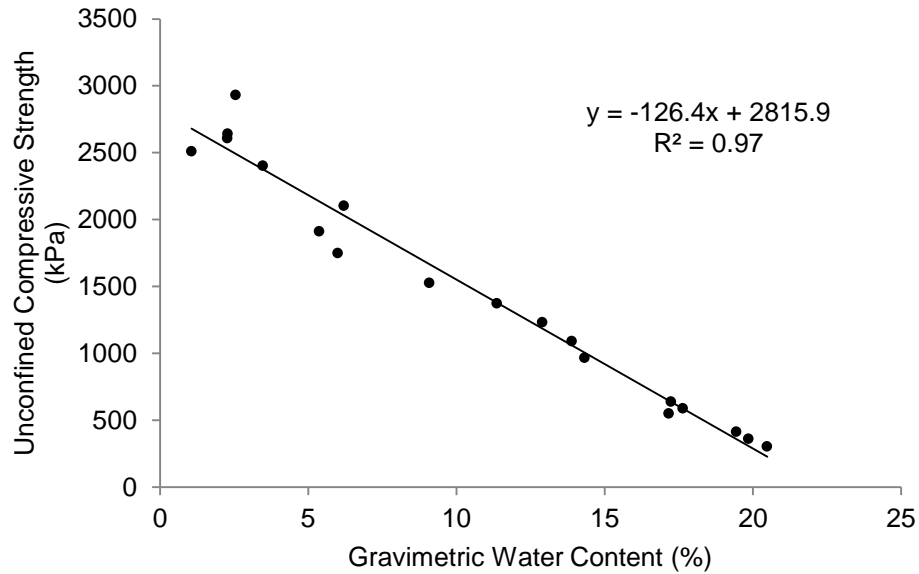


Fig. 12 Unconfined compressive strength as a function of water content for glacial till.

In adopting the Mohr circle plotting convention, strengths obtained from the direct test represent the minimum principal stress, σ_3 component while the maximum principal stress, σ_1 , is assumed to be zero, given the free strain boundary of the test in the vertical direction. Eqs. (4) and (5) provide the principal stresses at the centre of the Brazilian disc where R is the disc radius (Li and Wong, 2013).

$$\sigma_3 = \sigma_\theta \approx -P/\pi Rt \quad 1$$

$$\sigma_1 = \sigma_r \approx 3P/\pi Rt \quad 2$$

Representative plots are provided in Fig. 13 and show two moisture conditions, 6% and 19%; these depict a lower and upper bound of the Brazilian tested specimens. It may be seen that the coincidence of the direct and indirectly measured tensile strength at very low water contents defines the curvilinear, tension portion of the Mohr failure envelope (Fig. 13a). However, it was consistently observed that at higher water contents, Brazilian testing overestimated the tensile stress at failure (Fig. 13b). This is thought to be due to the plastic deformation produced by the compression loading of the Brazilian disc where tensile failure is assumed post-shear failure. Application of the DIC technique, as previously discussed, identified the progressively broadening region of vertical straining and hence, for specimens of high water content, it seems unlikely that the initial mode of failure was tensile.

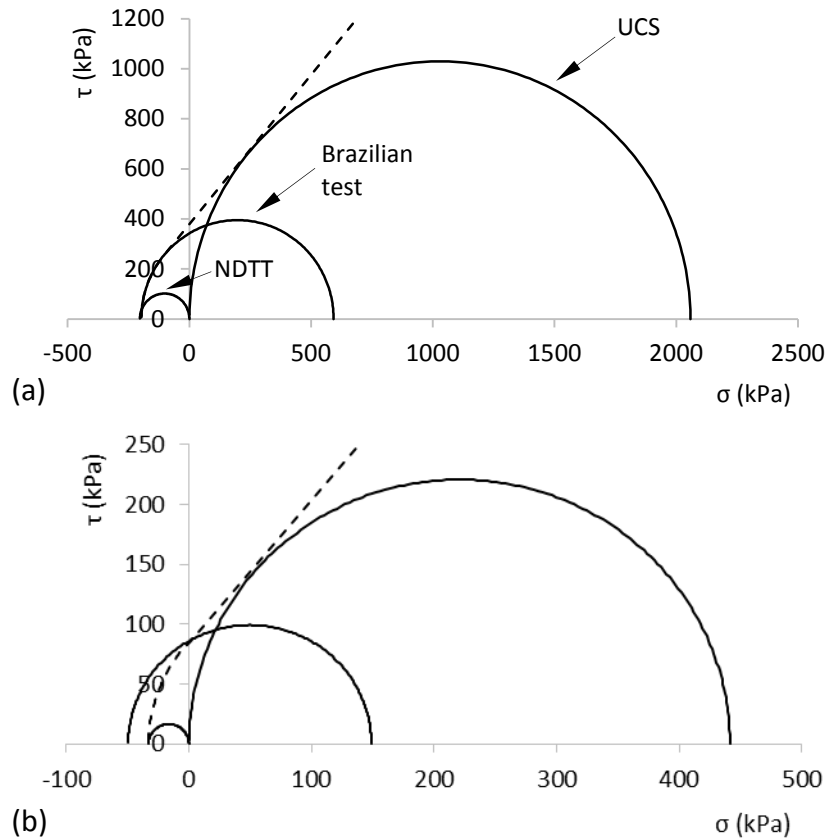


Fig. 13 Mohr circle plots depicting direct, Brazilian and UCS tests conducted on glacial till at (a) 6% and (b) 19% gravimetric water contents.

This analysis may be extrapolated to the KBS mix comparison data in Fig. 11 where a similar overestimation in tensile strength when tested indirectly is apparent at the higher water content. However, the cemented silty sand is found to show better consistency between the test methods at the higher water content than the other soils in Fig. 11. This may be explained by less plastic deformation during indirect testing brought about by the cemented soil having a lower plasticity and specimens being compacted and tested at water content considerably closer to the established optimum.

5 Conclusions

A testing methodology based on the adaptation of conventional direct shear testing apparatus has been demonstrated to provide a rigorous and repeatable means of measuring the tensile strength and stiffness behaviour of a range of geomaterials. The test can be used to assess changes in tensile strength with change in bulk moisture content at the ground surface or within the very near surface zone, where the majority of drying induced cracking initiates.

The use of artificially mixed material based on kaolin for its uniform composition and pale colour, allowed controllable and repeatable testing to be conducted with additional evaluation of the test performance at variable water contents and displacement rates via application of the Digital Image Correlation technique. The results of this study showed that at relatively high water contents, jaw-specimen contact was maintained throughout testing although jaw vertices influence the location of eventual failure. Conversely, at relatively low water contents, failure was induced at the constricted section following a period of specimen seating within the jaws. This technique has consistently provided evidence of tensile stress development in the absence of excessive compression/shearing leading to tensile failure of the specimen. Furthermore, a distinction has been drawn in the behaviour of clay soils with respect to the plastic limit where brittle crack propagation was observed in specimens $< P_l$ and a pronounced ductile trend at $> P_l$.

Brazilian testing was conducted on the same materials; however, limitations of the test restricted the conditions under which the materials could be tested. The need for brittle failure in Brazilian testing not only supports the development of the direct method but also brought about the need to validate the indirect soil testing. Once more, the DIC technique was able to provide a means of evaluating the failure conditions. A subsequent analytical procedure indicated the appropriate use of the classical Brazilian test calculation based upon a geometric ratio $y_1/a = 0.27$. However, in light of the DIC analysis, it is recommended that this be reduced to 0.20 as an upper boundary. This in turn reduces the range of applicable specimen saturation conditions to below the plastic limit of the tested material.

The dependency of water content on tensile behaviour of cohesive soils has been investigated and an exponential relationship has been identified. There is clear potential for this test to be used across a number of engineering applications where knowledge of the tensile strength of soils at the near surface is required, particularly when studying infiltration and stability issues in engineered and natural slopes as well as landfill capping layers.

Acknowledgements

The authors would like to acknowledge funding provided by the [iSMART \(EP/K027050/1\)](#) and [ATU \(EP/K021699/1\)](#) projects and also for the assistance in production of materials and testing from Jonathan Murphy, Chris Davies, Rosalind Hen-Jones and Paul Sargent. The XRD material characterisation of glacial till was conducted by S. Kemp and D. Wagner at the British Geological Survey. The authors are grateful to Yu-Jun Cui (ENPC, Paris) for his helpful comments on the production of this paper and to EU-COST Action [TU1202](#) that funded this exchange.

References

- Albrecht B.A. and Benson C.H., Effect of desiccation on compacted natural clays, *J. Geotech. Geoenviron.* **127** (1), 2001, 67–75.
- Alsayed M.I., Utilising the Hoek triaxial cell for multiaxial testing of hollow rock cylinders, *Int. J. Rock Mech. Min. Sci.* **39**, 2002, 355–366.
- Anderson M.G., Hubbard M.G. and Kneale P.E., The influence of shrinkage cracks on pore-water pressures within a clay embankment, *Q. J. Eng. Geol. Hydrogeol.* 1982, 9–14.
- Arslan H., Sture S. and Batiste S., Experimental simulation of tensile behaviour of lunar soil simulant JSC-1, *Mater. Sci. Eng.* **478** (1–2), 2008, 201–207.
- ASTM, Standard test method for splitting tensile strength of intact rock core specimens, In: *Annual Book of ASTM Standards*, 1984, 336–341.
- British Standard Institute, BS 1377-2: Methods for Test for Soils of Civil Engineering Purposes Part 2: Classification Tests, 1990a, BSI; Milton Keynes, UK.
- British Standard Institute, BS 1377-4: Methods of Test for Soils of Civil Engineering Purposes Part 4: Compaction-related Tests, 1990b, BSI; Milton Keynes, UK.
- British Standard Institute, BS 1377-7: Methods of Test for Soils for Civil Engineering Purposes Part 7: Shear Strength Tests (Total Stress), 1990c, BSI; Milton Keynes, UK.
- Chu T., Ranson W. and Sutton M., Applications of digital-image-correlation techniques to experimental mechanics, *Exp. Mech.* **25**, 1985, 232–244.
- Correlated Solutions, *Vic-3D Testing Guide*, 2010.

Corte, a. and Higashi, A. (1960). Experimental research on desiccation cracks in soil. U.S. Army Snow Ice and Permafrost Research Establishment, Research Report No. 66, Corps of Engineers, Wilmette, Illinois, U.S.A.

Davies C., Evaluation of the ST Tensile Testing Equipment for Use on Cohesive Soils Using Digital Imaging Correlation Technology, Newcastle University MSc Thesis, 2012, Newcastle, UK.

Dijkstra T.A. and Dixon N., Climate change and slope stability: challenges and approaches, *Q. J. Eng. Geol. Hydrogeol.* **43** (4), 2010, 371–385.

Divya P.V., Viswanadham B.V.S. and Gourc J.P., Evaluation of tensile strength–strain characteristics of fiber-reinforced soil through laboratory tests, *J. Mater. Civ. Eng.* **26** (1), 2014, 14–23.

Frydman S., The applicability of the Brazilian (indirect tension) test of soils, *Aust. J. Appl. Sci.* **15**, 1964, 335–343.

Groisman A. and Kaplan E., An experimental study of cracking induced by desiccation, *Europhys. Lett.* **25** (6), 1994, 415–420.

Heibrock G., Zeh R.M. and Witt K.J., Tensile strength of compacted clays, In: Schanz T., (Ed), *Unsaturated Soils: Experimental Studies*, 2005, Springer; Berlin Heidelberg, 395–412.

Hulme M., Jenkins G.J., Lu X., Turnpenny J.R., Mitchell T.D., Jones R.G., Lowe J., Murphy J.M., Hassell D., Boorman P., McDonald R. and Hill S., *Climate Change Scenarios for the United Kingdom: The UKCIP02 Scientific Report*, 2002, Tyndall Centre for Climate Change Research, School of Environmental Sciences, University of East Anglia; Norwich, UK, 120.

IMERYYS, Polwhite E — Data Sheet DAT020K, 2008, (Par, Cornwall, UK).
Jenkins G., Murphy J., Sexton D., Lowe J., Jones P. and Kilsby C., *UK Climate Predictions Briefing Report*, 2010, UK Climates Impacts Programme.

Jessberger H.L. and Stone K.J.L., Subsidence effects on clay barriers, *Geotechnique* **41** (2), 1991, 185–194.

Jones L.D. and Jefferson I., Expansive soils, In: Burland J., Chapman T., Skinner H. and Brown M., (Eds.), *ICE Manual of Geotechnical Engineering. Volume I: Geotechnical Engineering Principles, Problematic Soils and Site Investigation*, 2012, ICE Publishing; London, 413–441.

Kim, T. -H. & Hwang, C., 2003. Modeling of tensile strength on moist granular earth material at low water content. *Engineering Geology* 69, 233-244.

Kim T.H. and Sture S., Capillary induced tensile strength in unsaturated sands, *Can. Geotech. J.* **45** (5), 2008, 726–737.

Krishnayya A.V.G. and Einsenstein Z., Brazilian tensile test for soils, *Can. Geotech. J.* **11**, 1974, 632–642.

Lakshmikantha M.R., Prat P.C. and Ledesma A., Experimental evidence of size effect in soil cracking, *Can. Geotech. J.* **49**, 2012, 264–284.

Li D. and Wong L.N.Y., The Brazilian disc test for rock mechanics applications: review and new insights, *J. Rock Mech. Rock Eng.* **46**, 2013, 269–287.

Lu N., Wu B. and Tan C.P., Tensile strength characteristics of unsaturated sands, *J. Geotech. Geoenviron.* **133** (2), 2007, 144–154.

Nahlawi H., Chakrabarti S. and Kodikara J., A direct tensile strength testing method for unsaturated geomaterials, *Geotech. Test. J.* **27** (4), 2004, 1–6.

Peron H., Hueckel L., Laloui L. and Hu L.B., Fundamentals of desiccation cracking of fine-grained soils: experimental characterisation and mechanisms identification, *Can. Geotech. J.* **46**, 2009, 117–1201.

Philip L.K., Shimell H., Hewitt P.J. and Ellard H.T., A field-based test cell examining clay desiccation in landfill liners, *Q. J. Eng. Geol. Hydrogeol.* **35**, 2002, 345–354.

Rodriguez, R., 2002. Estudio experimental de flujo y transporte de cromo, níquel y manganeso en residuos de la zona minera de Moa (Cuba): Influencia del comportamiento hidromecánico. PhD Thesis. Technical University of Catalonia (UPC), Barcelona, Spain.

Romkens M.J.M. and Prasad S.N., Rain infiltration into swelling/shrinking/cracking soils, *Agric. Water Manag.* **86**, 2006, 196–205.

Stirling R.A., Simpson D.J. and Davie C.T., The application of digital image correlation to Brazilian testing of sandstone, *Int. J. Rock Mech. Min. Sci.* **60**, 2013, 1–11.

Stirling R.A., Hughes P.N., Davie C.T. and Glendinning S., Cyclic relationship between saturation and tensile strength in the near-surface zone of infrastructure embankments, In: Khalili K., Russell A. and Koshghalb A., (Eds.), *Unsaturated Soils: Research and Applications*, 2014, CRC Press; London, 1501–1505.

Tamrakar S.B., Toyosawa Y., Mitachi T. and Itoh K., Tensile strength of compacted and saturated soils using newly developed tensile strength measuring apparatus, *Soils Found.* **45** (6), 2005, 103–110.

Tang G.X. and Graham J., A method for testing tensile strength in unsaturated soils, *Geotech. Test. J.* **23** (3), 2000, 377–382.

Thusyanthan N.I., Take W.A., Madabhushi S.P.G. and Bolton M.D., Crack initiation in clay observed in beam bending, *Geotechnique* **57** (7), 2007, 581–594.

Trabelsi H., Jamei M., Zenzri H. and Olivella S., Crack patterns in clayey soils: experiments and modeling, *Int. J. Numer. Anal. Methods Geomech.* **36**, 2012, 1410–1433.

Wang Q.Z. and Xing L., Determination of fracture toughness K_{IC} by using the flattened Brazilian disc specimen for rocks, *Eng. Fract. Mech.* **64**, 1999, 193–201.

Zeh R.M. and Witt K.J., The tensile strength of compacted clays as affected by suction and soil structure, In: Schanz T., (Ed), *Experimental Unsaturated Soil Mechanics*, 2007, Springer; Berlin Heidelberg, 219–226.

Zhan T., Ng C. and Fredlund D.G., Instrumentation of an unsaturated expansive soil slope, *Geotech. Test. J.* **30** (2), 2006, 1–11.